



## Structure and frustrated magnetism of the two-dimensional triangular lattice antiferromagnet $\text{Na}_2\text{BaNi}(\text{PO}_4)_2$

Fei Ding(丁飞), Yongxiang Ma(马雍翔), Xiangnan Gong(公祥南), Die Hu(胡蝶), Jun Zhao(赵俊), Lingli Li(李玲丽), Hui Zheng(郑慧), Yao Zhang(张耀), Yongjiang Yu(于永江), Lichun Zhang(张立春), Fengzhou Zhao(赵凤周), and Bingying Pan(泮丙营)

**Citation:** Chin. Phys. B, 2021, 30 (11): 117505. DOI: 10.1088/1674-1056/abff1d

Journal homepage: <http://cpb.iphy.ac.cn>; <http://iopscience.iop.org/cpb>

**What follows is a list of articles you may be interested in**

---

### Crystal growth and magnetic properties of quantum spin liquid candidate $\text{KErTe}_2$

Weiwei Liu(刘维维), Dayu Yan(闫大禹), Zheng Zhang(张政), Jianting Ji(籍建亭), Youguo Shi(石友国), Feng Jin(金峰), and Qingming Zhang(张清明)

Chin. Phys. B, 2021, 30 (10): 107504. DOI: 10.1088/1674-1056/ac1574

### Effective model for rare-earth Kitaev materials and its classical Monte Carlo simulation

Mengjie Sun(孙梦杰), Huihang Lin(林慧航), Zheng Zhang(张政), Yanzhen Cai(蔡焱桢), Wei Ren(任玮), Jing Kang(康靖), Jianting Ji(籍建亭), Feng Jin(金峰), Xiaoqun Wang(王孝群), Rong Yu(俞榕), Qingming Zhang(张清明), and Zhengxin Liu(刘正鑫)

Chin. Phys. B, 2021, 30 (8): 087503. DOI: 10.1088/1674-1056/ac0a5d

### Some experimental schemes to identify quantum spin liquids

Yonghao Gao(高永豪), Gang Chen(陈钢)

Chin. Phys. B, 2020, 29 (9): 097501. DOI: 10.1088/1674-1056/ab9df0

### Typicality at quantum-critical points

Lu Liu(刘录), Anders W Sandvik, Wenan Guo(郭文安)

Chin. Phys. B, 2018, 27 (8): 087501. DOI: 10.1088/1674-1056/27/8/087501

### Monte Carlo study of the magnetic properties of spin liquid compound $\text{NiGa}_2\text{S}_4$

Zhang Kai-Cheng, Li Yong-Feng, Liu Yong, Chi Feng

Chin. Phys. B, 2014, 23 (5): 057501. DOI: 10.1088/1674-1056/23/5/057501

---

# Structure and frustrated magnetism of the two-dimensional triangular lattice antiferromagnet $\text{Na}_2\text{BaNi}(\text{PO}_4)_2$ \*

Fei Ding(丁飞)<sup>1</sup>, Yongxiang Ma(马雍翔)<sup>1</sup>, Xiangnan Gong(公祥南)<sup>2</sup>, Die Hu(胡蝶)<sup>3</sup>, Jun Zhao(赵俊)<sup>3</sup>, Lingli Li(李玲丽)<sup>4</sup>, Hui Zheng(郑慧)<sup>4</sup>, Yao Zhang(张耀)<sup>4</sup>, Yongjiang Yu(于永江)<sup>1</sup>, Lichun Zhang(张立春)<sup>1</sup>, Fengzhou Zhao(赵凤周)<sup>1</sup>, and Bingying Pan(泮丙莹)<sup>1,†</sup>

<sup>1</sup>School of Physics and Optoelectronic Engineering, Ludong University, Yantai 264025, China

<sup>2</sup>Analytical and Testing Center, Chongqing University, Chongqing 401331, China

<sup>3</sup>State Key Laboratory of Surface Physics, Department of Physics, and Advanced Materials Laboratory, Fudan University, Shanghai 200433, China

<sup>4</sup>School of Chemistry and Materials Science, Ludong University, Yantai 264025, China

(Received 24 January 2021; revised manuscript received 15 April 2021; accepted manuscript online 8 May 2021)

A new frustrated triangular lattice antiferromagnet  $\text{Na}_2\text{BaNi}(\text{PO}_4)_2$  was synthesized by high temperature flux method. The two-dimensional triangular lattice is formed by the  $\text{Ni}^{2+}$  ions with  $S = 1$ . Its magnetism is highly anisotropic with the Weiss constants  $\theta_{\text{CW}} = -6.615$  K ( $H \perp c$ ) and  $-43.979$  K ( $H \parallel c$ ). However, no magnetic ordering is present down to 0.3 K, reflecting strong geometric spin frustration. Our heat capacity measurements show substantial residual magnetic entropy existing below 0.3 K at zero field, implying the presence of low energy spin excitations. These results indicate that  $\text{Na}_2\text{BaNi}(\text{PO}_4)_2$  is a potential spin liquid candidate with spin-1.

**Keywords:** frustrated magnetism, spin liquid, triangle lattice

**PACS:** 75.10.Kt, 75.50.Ee, 75.10.Jm

**DOI:** 10.1088/1674-1056/abff1d

## 1. Introduction

The frustrated triangular lattice antiferromagnets (FTLAs) have been widely studied for their relation to quantum spin liquid (QSL) states.<sup>[1–4]</sup> The well-known  $S = 1/2$  QSL material candidates include the FTLAs like  $\text{EtMe}_3\text{Sb}[\text{Pd}(\text{dmit})_2]_2$ ,<sup>[5,6]</sup>  $\kappa\text{-(BEDT-TTF)}_2\text{Cu}_2(\text{CN})_3$ ,<sup>[7,8]</sup> and  $\text{YbMgGaO}_4$ .<sup>[9]</sup> Spin liquid states may also be realized on  $S = 1$  FTLAs such as in  $\text{Ba}_3\text{NiSb}_2\text{O}_9$ .<sup>[10]</sup> Furthermore, the competition of magnetic interactions in FTLA leads to complex phenomena like topological transitions,<sup>[11]</sup> the 1/3-magnetization plateau in  $\text{Cs}_2\text{CuBr}_4$ ,<sup>[12,13]</sup> and the successive phase transitions in  $\text{CsNiBr}_3$ .<sup>[14]</sup> However, real FTLA materials often suffer with problems from lattice distortion and interlayer interactions, so structurally perfect FTLAs are still highly desirable.<sup>[15]</sup>

Recently, there are reports of FTLA materials in which separated  $\text{MO}_6$  ( $M$  = transition metal ions) octahedra form a perfect two-dimensional triangular lattice.<sup>[16,17]</sup> The octahedra do not share any oxygen atom with each other, making the antiferromagnetic interactions moderate. For example, in the spin liquid candidate  $\text{Na}_2\text{BaCo}(\text{PO}_4)_2$ , the triangular lattice is formed by separated  $\text{CoO}_6$  octahedra.<sup>[16]</sup> Similar layered triangular lattice structures were observed in  $\text{A}\text{Ag}_2\text{M}[\text{VO}_4]_2$  ( $A = \text{Ba}, \text{Sr}$ ;  $M = \text{Co}, \text{Ni}$ )<sup>[18]</sup> and  $\text{Na}_2\text{BaMV}_2\text{O}_8$  ( $M = \text{Ni}, \text{Mn}, \text{Co}$ ),<sup>[17]</sup> but these compounds are ferromagnets except for

$\text{Na}_2\text{BaMnV}_2\text{O}_8$ .<sup>[17]</sup> The distinct magnetic properties of these triangular lattice magnets largely stem from the subtle octahedron crystal field environment and superexchange coupling pathways. It is of great interest to explore related materials to search for structurally perfect FTLAs.

Here, we report the structure and magnetic properties of a new FTLA material  $\text{Na}_2\text{BaNi}(\text{PO}_4)_2$ . The crystal has a layered magnetic structure. The  $\text{Ni}^{2+}$  ions with  $S = 1$  form a perfect triangular lattice within the magnetic layers and shows antiferromagnetic magnetism. Its magnetization is highly anisotropic between  $\chi_{\parallel}$  and  $\chi_{\perp}$ , demonstrating strong easy-plane type anisotropy. Although its Weiss constants are  $\theta_{\text{CW}} = -6.615$  K ( $H \perp c$ ) and  $-43.979$  K ( $H \parallel c$ ), no magnetic ordering is observed down to 0.3 K. We also find substantial residual magnetic entropy at zero field. These results reveal the highly frustrated magnetism in  $\text{Na}_2\text{BaNi}(\text{PO}_4)_2$ .

## 2. Experiment

### 2.1. Synthesis

Single crystals of  $\text{Na}_2\text{BaNi}(\text{PO}_4)_2$  were synthesized by the flux method. First, 4 mmol  $\text{BaCO}_3$  (99.99%, Adamas), 4 mmol  $\text{NiO}$  (99%, Aldrich), 8 mmol  $(\text{NH}_4)_2\text{HPO}_4$  (99%, Adamas), and 60 mmol  $\text{NaCl}$  (99.5%, Greagent) flux media were fully mixed. The mixture was loaded into a 10 mL alumina crucible, capped with a lid, and heated up in a box-type

\*Project supported by the National Natural Science Foundation of China (Grant No. 11804137) and the Natural Science Foundation of Shandong Province, China (Grant Nos. ZR2020YQ03 and ZR2018BA026).

†Corresponding author. E-mail: bypan@ldu.edu.cn

furnace. After staying at 950 °C for 2 hours, it was cooled to 750 °C at a rate of 3°C/h, and then naturally cooled to room temperature. The obtained crystals were washed in water and separated.

## 2.2. Single crystal x-ray diffraction

Single crystal x-ray diffraction at 293 K was performed by the Agilent SuperNova diffractometer (Mo  $K\alpha$  radiation,  $\lambda = 0.71073$  Å). We used the CrysAlisPro program for x-ray data collection, reduction, and absorption corrections. The SHELXL program package was employed to solve the crystal structure via the direct method.<sup>[19,20]</sup>

## 2.3. Magnetic susceptibility and heat capacity measurement

The direct-current (DC) magnetic susceptibility measurements were conducted by a MPMS SQUID magnetometer

(Quantum Design) with field applied perpendicular or parallel to the  $c$  axis. The heat capacity was measured by a physical property measurement system (PPMS, Quantum Design) with a dilution refrigerator insert in magnetic fields up to 9 T.

## 3. Results and discussion

The synthesized hexagonal plate-like single crystals of  $\text{Na}_2\text{BaNi}(\text{PO}_4)_2$  are shown in Fig. 1(a). Single crystal structure determination and refinement indicate that the compound crystallizes in a trigonal structure with the space group  $P\bar{3}$ . The lattice constants are  $a = b = 5.2790(3)$  Å and  $c = 6.9596(4)$  Å. Detailed crystal refinement data and atomic coordinates are listed in Tables 1 and 2. It should be noted that our single crystal diffraction did not show detectable site mixing as appeared in some low-dimensional magnets. Crystallographic data of  $\text{Na}_2\text{BaNi}(\text{PO}_4)_2$  has been deposited at the Cambridge Crystallographic Data Center (CCDC 2040965).

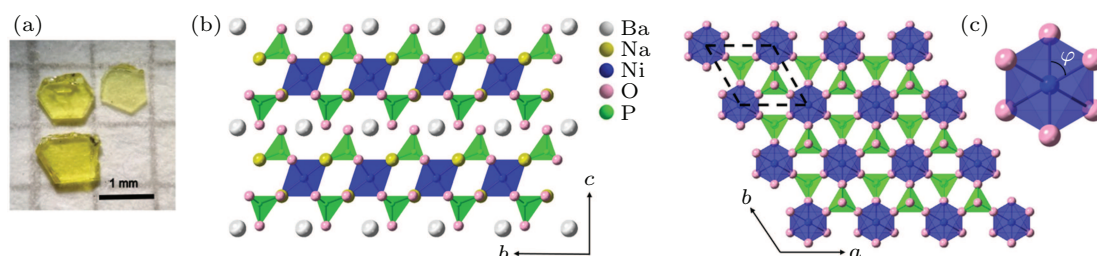


**Fig. 1.** Crystal structure of  $\text{Na}_2\text{BaNi}(\text{PO}_4)_2$ . (a) Yellow-colored crystals with hexagonal plate-like shape. (b) Layered structure with two-dimensional  $\text{NiO}_6$  octahedra stacking along the  $c$  axis. (c) Triangular magnetic lattice in the  $ab$  plane. Right panel:  $\text{NiO}_6$  octahedron unit with  $\varphi = 93.1(6)^\circ$ .

**Table 1.** Crystal data and structure refinement for  $\text{Na}_2\text{BaNi}(\text{PO}_4)_2$ .

Empirical formula	$\text{Na}_2\text{BaNi}(\text{PO}_4)_2$
Formula weight	431.94
Temperature	293(2)
Wavelength	0.71073 Å
Crystal system	trigonal
Space group	$P\bar{3}$
Unit cell dimensions	$a = 5.2790(3)$ Å $b = 5.2790(3)$ Å $c = 6.9596(4)$ Å $\alpha = \beta = 90^\circ$ $\gamma = 120^\circ$
Cell volume	$167.96(2)$ Å <sup>3</sup>
Z	1
Calculated density	$4.271$ g/cm <sup>3</sup>
$F(000)$	200.0
$2\theta$ range for data collection	$8.914^\circ$ to $57.938^\circ$
Index ranges	$-6 \leq h \leq 3$ , $0 \leq k \leq 6$ , $0 \leq l \leq 9$
Reflections collected	266
Data/restraints/parameters	266/0/25
Final $R$ indexes [ $I \geq 2\sigma(I)$ ]	$R_1 = 0.0446$ $wR_2 = 0.1152$
Final $R$ indexes [all data]	$R_1 = 0.0465$ $wR_2 = 0.1169$
Goodness-of-fit on $F^2$	1.102

**Table 2.** Atomic coordinates and equivalent isotropic displacement parameters (Å<sup>2</sup>) for  $\text{Na}_2\text{BaNi}(\text{PO}_4)_2$ .

Atom	$x$	$y$	$z$	$U(\text{eq})^a$
Ba01	10000	10000	5000	9.7(6)
Ni02	10000	10000	0	8.0(7)
P003	3333.33	6666.67	2563(4)	4.4(8)
Na04	3333.33	6666.67	8201(9)	13.5(12)
O005	3333.33	6666.67	4730(12)	8.6(17)
O006	6422(12)	7733(13)	1793(7)	13.4(15)

<sup>a</sup> $U(\text{eq})$  is 1/3 of the trace of the  $U_{ij}$  tensor.

The resulted crystal structure of  $\text{Na}_2\text{BaNi}(\text{PO}_4)_2$  is illustrated in Figs. 1(b) and 1(c).  $\text{Ni}^{2+}$  ions ( $S = 1$ ) form two-dimensional triangular lattice layers well separated by the non-magnetic  $(\text{PO}_4)^{3-}$ ,  $\text{Ba}^{2+}$ , and  $\text{Na}^+$  ions. The magnetic layers follow a simple A–A–A stacking mode along the  $c$  axis (Fig. 1(b)). Each  $\text{Ni}^{2+}$  ion coordinates with six nearest oxygen atoms to form an octahedron, as shown in the right panel of Fig. 1(c). Within the  $\text{NiO}_6$  octahedron, the Ni–O bond lengths are  $2.050(17)$  Å. The octahedron distortion can be characterized by the bond angle  $\varphi$  defined in Fig. 1(c) which is  $93.1(6)^\circ$  for  $\text{Na}_2\text{BaNi}(\text{PO}_4)_2$ , the extent of distortion is similar to that in  $\text{Na}_2\text{BaMV}_2\text{O}_8$  ( $M = \text{Ni}, \text{Mn}, \text{Co}$ ).<sup>[17]</sup> There is no shared edge or corner between the  $\text{NiO}_6$  octahedra and the magnetic interactions between the spins in the triangular lattice propagate along the  $\text{Ni}[\text{PO}_4]\text{Ni}$  pathway, which should lead to mod-

erate superexchange as observed in related materials.<sup>[16–18]</sup> In contrast, the interlayer superexchange is along the Ni–[PO<sub>4</sub>]–[PO<sub>4</sub>–Ni pathway (Fig. 1(b)) which should be much smaller than the intralayer interaction, making the system a two-dimensional magnet.

DC magnetic susceptibility ( $\chi$ ) of the Na<sub>2</sub>BaNi(PO<sub>4</sub>)<sub>2</sub> single crystal was measured from 2 K to 300 K with an external field of  $H = 1000$  Oe. The field was applied either perpendicular or parallel to the  $c$  axis. As can be seen in Fig. 2,  $\chi_{\perp}$  and  $\chi_{\parallel}$  monotonically increase with lowering temperature, without any signature of phase transitions down to 2 K. The field-cooling (black squares) and zero-field-cooling (ZFC) (green dashed line) data overlap with each other in the measured temperature range (Fig. 2(a)), excluding the spin glass state. The Curie–Weiss law  $1/\chi = (T - \theta_{\text{CW}})/C$  was used to fit the data between 50 K and 300 K for  $1/\chi_{\perp}$ , as indicated by the red lines in Fig. 2(a).  $1/\chi_{\parallel}$ , however, deviates from the Curie–Weiss law below 100 K, so the data between 100 K and 300 K were used for fitting (Fig. 2(b)). The fitting results are  $\theta_{\text{CW},\perp} = -6.615$  K,  $C_{\perp} = 1.195$  emu·K/mol and  $\theta_{\text{CW},\parallel} = -43.979$  K,  $C_{\parallel} = 1.836$  emu·K/mol for  $\chi_{\perp}(T)$  and  $\chi_{\parallel}(T)$ , respectively. The negative Weiss constants indicate that the dominate exchange in Na<sub>2</sub>BaNi(PO<sub>4</sub>)<sub>2</sub> is antiferromagnetic. This is in sharp contrast with its analogous compound Na<sub>2</sub>BaNi(VO<sub>4</sub>)<sub>2</sub> which is a ferromagnet with a transition temperature at 8.4 K.<sup>[17]</sup>

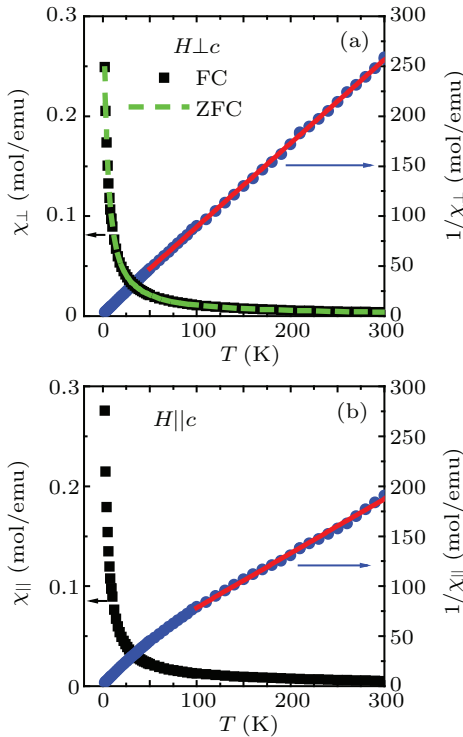


**Fig. 2.** Magnetic susceptibility of Na<sub>2</sub>BaNi(PO<sub>4</sub>)<sub>2</sub> with field (a) perpendicular and (b) parallel to  $c$ . The FC data (black squares) and ZFC data (green dashed line) were measured under  $H = 1000$  Oe and in the temperature range from 2 K to 300 K. The red solid lines are the Curie–Weiss law fittings for the  $1/\chi(T)$  data (blue dots).

The significant difference between  $\theta_{\text{CW},\perp}$  and  $\theta_{\text{CW},\parallel}$  re-

veals strong magnetic anisotropy in Na<sub>2</sub>BaNi(PO<sub>4</sub>)<sub>2</sub> which reflects strong anisotropic exchange interactions in its spin Hamiltonian. Similar anisotropic magnetism has been found in related layered magnets like Na<sub>2</sub>BaMV<sub>2</sub>O<sub>8</sub> ( $M = \text{Ni, Mn, Co}$ ),<sup>[17]</sup> BaCo<sub>2</sub>(AsO<sub>4</sub>)<sub>2</sub>,<sup>[21]</sup> and  $\alpha$ -RuCl<sub>3</sub>.<sup>[22]</sup> To further reveal the magnetic anisotropy, we measured magnetization at  $T = 300$  K, 100 K, 50 K, and 2 K with field perpendicular or parallel to the  $c$  axis, the results are shown in Fig. 3. In Figs. 3(a)–3(d), both  $M_{\parallel}$  and  $M_{\perp}$  increase linearly from 0 to 7 T with  $M_{\parallel}$  apparently larger than  $M_{\perp}$ . The anisotropy can still be observed at 300 K (Fig. 3(a)), indicating the anisotropic excitation gap should be comparable to the thermal energy.

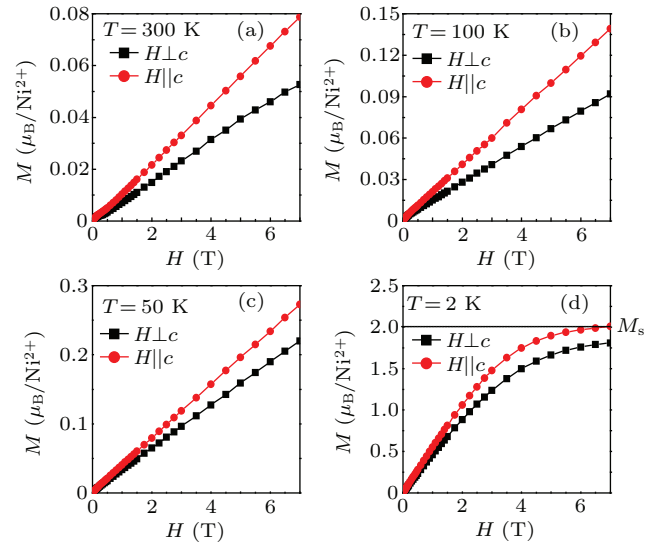


**Fig. 3.** Magnetization at (a) 300 K, (b) 100 K, (c) 50 K, and (d) 2 K. The dotted line in (d) indicates the saturated magnetization value for a Ni<sup>2+</sup> ion when only considering the spin moment.

At 2 K,  $M$  is proportional to  $H$  at lower fields and tends to saturate at high fields (Fig. 3(d)). The theoretical saturated magnetization  $M_s$  is  $gS\mu_B$ .  $M_s$  equals to  $2 \mu_B/\text{Ni}^{2+}$  if only considering the spin moment, consistent with the observed value. The magnetization curves at all measured temperatures have no anomaly, indicating absence of magnetic transitions or long range orderings. The 1/3 magnetization plateau stemming from quantum spins in a triangular lattice is also absent here, implying that Na<sub>2</sub>BaNi(PO<sub>4</sub>)<sub>2</sub> may be treated as a classic FTLA.

The heat capacity data of Na<sub>2</sub>BaNi(PO<sub>4</sub>)<sub>2</sub> at magnetic fields up to 9 T are presented in Fig. 4. The heat capacity above 30 K is field independent and does not show any anomaly related to phase transitions (Fig. 4(a)). However, the low temperature data exhibit a broad peak that shifts to higher temperatures with stronger fields (Fig. 4(b)). This feature is typical in several  $S = 1$  QSL candidates such as [NH<sub>4</sub>]<sub>2</sub>[C<sub>7</sub>H<sub>14</sub>N][V<sub>7</sub>O<sub>6</sub>F<sub>18</sub>]<sup>[23]</sup> and Ba<sub>3</sub>NiSb<sub>2</sub>O<sub>9</sub>.<sup>[10]</sup> Some  $S = 1/2$  QSL candidates such as YbMgGaO<sub>4</sub> and Na<sub>2</sub>BaNi(PO<sub>4</sub>)<sub>2</sub> also exhibit similar broad feature in heat capacity at low temperature.<sup>[9,16]</sup>



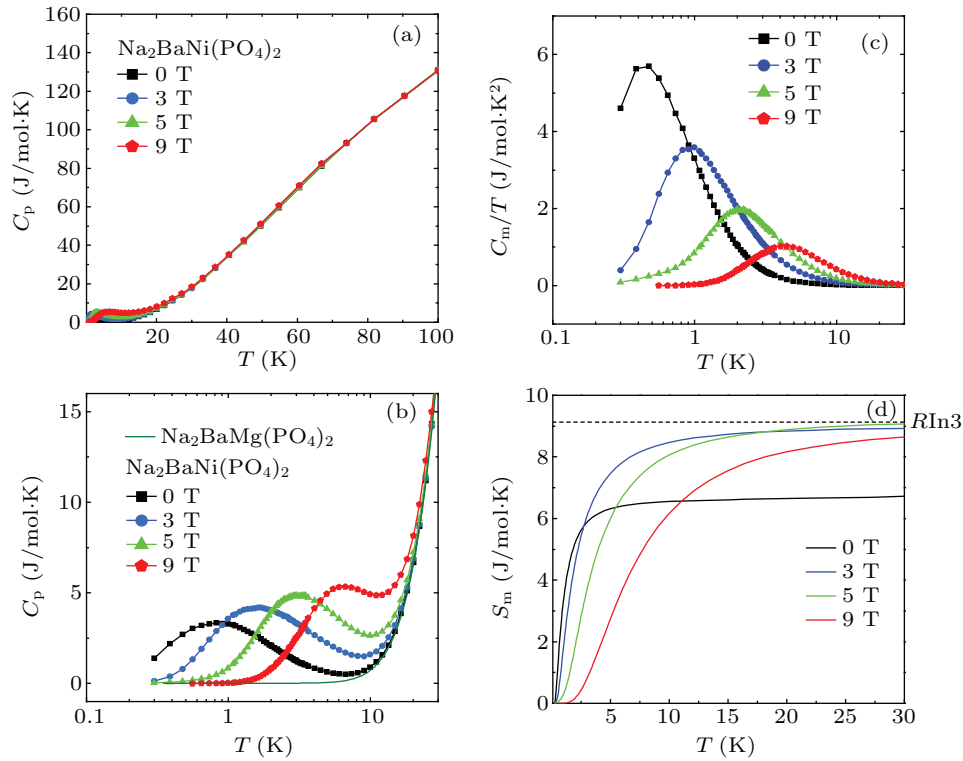


**Fig. 4.** (a) Heat capacity of  $\text{Na}_2\text{BaNi}(\text{PO}_4)_2$  below 100 K. (b) Heat capacity in the temperature range from 0.3 K to 30 K. The magnetic fields are at 0 T, 3 T, 5 T, and 9 T respectively. The heat capacity of  $\text{Na}_2\text{BaMg}(\text{PO}_4)_2$  (olive solid line) was obtained from Ref. [16]. (c) Temperature dependences of  $C_m/T$  at different fields. (d) Integrated magnetic entropy  $S_m$  of  $\text{Na}_2\text{BaNi}(\text{PO}_4)_2$ .  $R\ln 3$  is the total magnetic entropy for an  $S = 1$  magnet.

Magnetic heat capacity  $C_m$  is sensitive to the low energy spin excitations. We used the heat capacity of  $\text{Na}_2\text{BaMg}(\text{PO}_4)_2$  as the phonon contribution in  $\text{Na}_2\text{BaNi}(\text{PO}_4)_2$  since they are isostructural (solid line in Fig. 4(b), the data was obtained from Ref. [16]). The temperature dependences of  $C_m/T$  at different fields are displayed in Fig. 4(c). The magnetic entropy  $S_m(T)$  was subsequently obtained by integrating  $C_m/T$  from  $\sim 0.3$  K to  $T$  (Fig. 4(d)). For an  $S = 1$  magnet, the total magnetic entropy is  $R\ln 3$ , where  $R$  is the ideal gas constant. As can be seen in Fig. 4(d),  $S_m$  is nearly saturated by 30 K. The zero field magnetic entropy is only  $0.74R\ln 3$  at 30 K, indicating substantial residual magnetic entropy below 0.3 K. The zero point entropy usually comes from strong spin fluctuations in disordered systems which lift the degeneracy of the ground state. By applying a magnetic field, the energy barriers of spin reorientations will be enhanced, making  $S_m$  increase to its conventional value  $R\ln 3$ , consistent with our experimental observed value at magnetic fields (Fig. 4(d)).

It is interesting to compare  $\text{Na}_2\text{BaNi}(\text{PO}_4)_2$  with its analog compound  $\text{Na}_2\text{BaCo}(\text{PO}_4)_2$ , the Co-based triangular lattice antiferromagnet.<sup>[16]</sup> Both compounds have the  $\text{MO}_6\text{--PO}_4\text{--PO}_4\text{--MO}_6$  ( $M = \text{Ni, Co}$ ) stacking structure along the  $c$  axis. Their lattice constants only have slight differences. For instance, the closest Ni–Ni distance is 5.279 Å in  $\text{Na}_2\text{BaNi}(\text{PO}_4)_2$  and the closest Co–Co distance is 5.319 Å in  $\text{Na}_2\text{BaCo}(\text{PO}_4)_2$ . The similarities in structure result in moderate antiferromagnetic couplings in both compounds. However, the magnetic anisotropy in  $\text{Na}_2\text{BaCo}(\text{PO}_4)_2$  is insignificant

with  $\Theta_{\text{CW},\perp} = -31.9$  K and  $\Theta_{\text{CW},\parallel} = -32.6$  K, in sharp contrast with the strong magnetic anisotropy in  $\text{Na}_2\text{BaNi}(\text{PO}_4)_2$ . The anisotropy is closely related to the angular distributions of the outmost 3d electron orbits and largely depends on the 3d electron configurations as well as the octahedra crystal field. Further study by inelastic neutron scattering on  $\text{Na}_2\text{BaNi}(\text{PO}_4)_2$  is necessary to determine its detailed exchange couplings and anisotropic spin Hamiltonian.

## 4. Conclusion

In summary, we have synthesized a new antiferromagnet  $\text{Na}_2\text{BaNi}(\text{PO}_4)_2$ . From single crystal x-ray diffraction we find that its crystal structure has a perfect two-dimensional triangular lattice formed by  $\text{Ni}^{2+}$  ions. The Weiss constants are  $-6.615$  K and  $-43.979$  K for field perpendicular and parallel to the  $c$  axis, respectively. However, magnetic ordering is absent down to 0.3 K and up to 9 T. So we conclude that  $\text{Na}_2\text{BaNi}(\text{PO}_4)_2$  is a new FLTA that could be used for study of novel states such as QSL in frustrated magnets.

## References

- [1] Balents L 2010 *Nature* **464** 199
- [2] Broholm C, Cava R J, Kivelson S A, Nocera D G, Norman M R and Senthil T 2020 *Science* **367** eaay0668
- [3] Ma Z, Ran K, Wang J, Bao S, Cai Z, Li S and Wen J 2018 *Chin. Phys. B* **27** 106101
- [4] Gao Y H and Chen G 2020 *Chin. Phys. B* **29** 097501
- [5] Itou T, Oyama A, Maegawa S and Kato R 2010 *Nat. Phys.* **6** 673
- [6] Yamashita M, Nakata N, Senshu Y, Nagata M, Yamamoto H M, Kato R, Shibauchi T and Matsuda Y 2010 *Science* **328** 1246

- [7] Shimizu Y, Miyagawa K, Kanoda K, Maesato M and Saito G 2003 *Phys. Rev. Lett.* **91** 107001
- [8] Yamashita S, Yamamoto T, Nakazawa Y, Tamura M and Kato R 2011 *Nat. Commun.* **2** 275
- [9] Li Y, Liao H, Zhang Z, Li S, Jin F, Ling L, Zhang L, Zou Y, Pi L, Yang Z, Wang J, Wu Z and Zhang Q 2015 *Sci. Rep.* **5** 16419
- [10] Cheng J G, Li G, Balicas L, Zhou J S, Goodenough J B, Xu C and Zhou H D 2011 *Phys. Rev. Lett.* **107** 197204
- [11] Kawamura H, Yamamoto A and Okubo T 2010 *J. Phys. Soc. Jpn.* **79** 023701
- [12] Jason A, Chubukov Andrey V and Strykh Oleg A 2009 *Phys. Rev. Lett.* **102** 137201
- [13] Wei Z C, Liao H J, Chen J, Xie H D, Liu Z Y, Xie Z Y, Li W, Normand B and Xiang T 2016 *Chin. Phys. Lett.* **33** 077503
- [14] Maegawa S, Kohmoto T, Goto T and Fujiwara N 1991 *Phys. Rev. B* **44** 12617
- [15] Zhou Y, Kanoda K and Ng T K 2017 *Rev. Mod. Phys.* **89** 025003
- [16] Zhong R, Guo S, Xu G, Xu Z and Cava R J 2019 *Proc. Natl. Acad. Sci. USA* **116** 14505
- [17] Nakayama G, Hara S, Sato H, Narumi Y and Nojiri H 2013 *J. Phys. Condens. Matter* **25** 116003
- [18] Möller A, Amuneke N E, Daniel P, Lorenz B, de la Cruz, Clarina R, Gooch M and Chu P C W 2012 *Phys. Rev. B* **85** 214422
- [19] Dolomanov O V, Bourhis L J, Gildea R J, Howard J A K and Puschmann H 2009 *J. Appl. Cryst.* **42** 339
- [20] Sheldrick G M 2015 *Acta Cryst.* **71** 3
- [21] Zhong R, Gao T, Ong N P and Cava R J 2020 *Sci. Adv.* **6** eaay6953
- [22] Lampen-Kelley P, Rachel S, Reuther J, Yan J Q, Banerjee A, Bridges C A, Cao H B, Nagler S E and Mandrus D 2018 *Phys. Rev. B* **98** 100403
- [23] Clark L, Orain J C, Bert F, De Vries M A, Aidoudi F H, Morris R E, Lightfoot P, Lord J S, Telling M T F, Bonville P, Attfield J P, Mendels P and Harrison A 2013 *Phys. Rev. Lett.* **110** 207208
- [24] Kataoka K, Hirai D, Yajima T, Nishio-Hamane D, Ishii R, Choi K Y, Wulferding D, Lemmens P, Kittaka S, Sakakibara T, Ishikawa H, Matsuo A, Kindo K and Hiroi Z 2020 *J. Phys. Soc. Jpn.* **89** 114709